

GEANT4 simulation study of over-response phenomenon of fiber x-ray sensor

Bin Zhang(张彬), Tian-Ci Xie(谢天赐), Zhuang Qin(秦壮), Hao-Peng Li(李昊鹏), Song Li(李松), Wen-Hui Zhao(赵文辉), Zi-Yin Chen(陈子印), Jun Xu(徐军), Elfed Lewis, and Wei-Min Sun(孙伟民)

Citation: Chin. Phys. B, 2021, 30 (**4**): 048701. DOI: 10.1088/1674-1056/abcfa6
Journal homepage: http://cpb.iphy.ac.cn; http://iopscience.iop.org/cpb

What follows is a list of articles you may be interested in

Phase transition of DNA compaction in confined space: Effects of macromolecular crowding are dominant

Erkun Chen(陈尔坤), Yangtao Fan(范洋涛), Guangju Zhao(赵光菊), Zongliang Mao(毛宗良), Haiping Zhou(周海平), Yanhui Liu(刘艳辉)

Chin. Phys. B, 2020, 29 (**1**): 018701. DOI: 10.1088/1674-1056/ab5941

Application of microdosimetry on biological physics for ionizing radiation

Dandan Chen(陈丹丹), Liang Sun(孙亮)

Chin. Phys. B, 2018, 27 (**2**): 028701. DOI: 10.1088/1674-1056/27/2/028701

Thermal properties of a two-dimensional intrinsically curved semiflexible biopolymer

Zicong Zhou(周子聪), Yanting Wang(王延颋)

Chin. Phys. B, 2017, 26 (**3**): 038701. DOI: 10.1088/1674-1056/26/3/038701

Stretching instability of intrinsically curved semiflexible biopolymers: A lattice model approach

Zhou Zi-Cong, Lin Fang-Ting, Chen Bo-Han

Chin. Phys. B, 2015, 24 (**2**): 028701. DOI: 10.1088/1674-1056/24/2/028701

PET image reconstruction with a system matrix containing point spread function derived from single photon incidence response

Fan Xin, Wang Hai-Peng, Yun Ming-Kai, Sun Xiao-Li, Cao Xue-Xiang, Liu Shuang-Quan, Chai Pei, Li Dao-Wu, Liu Bao-Dong, Wang Lu, Wei Long

Chin. Phys. B, 2015, 24 (**1**): 018702. DOI: 10.1088/1674-1056/24/1/018702

GEANT4 simulation study of over-response phenomenon of fiber x-ray sensor*

Bin Zhang(张彬)[1], Tian-Ci Xie(谢天赐)[1], Zhuang Qin(秦壮)[2], Hao-Peng Li(李昊鹏)[1], Song Li(李松)[1], Wen-Hui Zhao(赵文辉)[1], Zi-Yin Chen(陈子印)[3], Jun Xu(徐军)[4], Elfed Lewis[5], and Wei-Min Sun(孙伟民)[1,†]

[1] *Key Laboratory of In-fiber Integrated Optics, Ministry of Education, Harbin Engineering University, Harbin* 150001, *China*
[2] *Electronic Engineering College, Ministry of Education, Heilongjiang University, Harbin* 150001, *China*
[3] *Comprehensive Cancer Center, First Affiliated Hospital of Harbin Medical University, Harbin* 150001, *China*
[4] *Comprehensive Cancer Center, Second Affiliated Hospital of Harbin Medical University, Harbin* 150001, *China*
[5] *Optical Fiber Sensors Research Centre, University of Limerick, Castletroy, Limerick, Ireland*

(Received 17 September 2020; revised manuscript received 4 November 2020; accepted manuscript online 2 December 2020)

The purpose of this article is to explore the cause of the over-response phenomenon of fiber x-ray sensor. The sensor is based on a length of PMMA fiber, whose end is filled with the scintillation material Gd_2O_2S:Tb. The Monte Carlo simulation software GEANT4 uses the phase space file provided by the International Atomic Energy Agency (IAEA), by irradiating the fiber x-ray sensor in the water phantom, counting the fluorescence signal of the optical fiber x-ray sensor after propagation through the fiber. In addition, the number of Cerenkov photons propagating through the fiber is also counted. Comparing this article with previous research, we believe that one of the reasons for the over-response of the fiber x-ray sensor is the non-linear response of the deposition energy of the scintillator to the fluorescence. By establishing a region of interest and counting the x-rays in this region, the simulation results show that the counted number of x-rays that may affect the fiber x-ray sensor is the biggest in the area of interest at a water depth of 5 cm. This result is close to the maximum dose point of the experimental and simulated percentage depth dose (PDD) curve of fiber x-ray sensor. Therefore, the second reason of the over-response phenomenon is believed to be fact that the inorganic materials such as Gd_2O_2S:Tb have larger effective atomic numbers, so the fiber x-ray sensors will cause more collisions with x-ray in a low energy region of 0.1 MeV–1.5 MeV.

Keywords: fiber x-ray sensors, over-response, percentage depth dose (PDD), Monte Carlo (MC) simulation

PACS: 87.10.Rt, 87.15.ak, 87.16.A– **DOI:** 10.1088/1674-1056/abcfa6

1. Introduction

Many new radiotherapy technologies have recently been developed including intensity modulated radiotherapy,[1] small field radiotherapy,[2] and real-time radiotherapy.[3] In many clinical radiotherapy treatments and quality assurance (QA) processes, the traditional ionization chamber (IC) device is used to calibrate and correct the dose delivery from a linear accelerator. During the development of sophisticated modern radiotherapy technology, a clear need existed for additional sensors to the IC which are miniaturized and could operate in real-time during beam delivery. The existence of the need for additional real-time clinical dosimeters has been a driver for the emergence of sensor devices based on several different technologies. Promising candidate technologies include thermoluminescent dosimeters (TLDs) and radiochromic films which possess excellent spatial resolution, but they are incapable of providing real-time measurement. They are also limited in their working life and sensitivity and at best require regular recalibration. The IC is considered to be the clinical gold standard detector, but cannot perform real-time detection *in-vivo* as it requires high voltage[4,5] for its operation. Fiber x-ray sensors have the advantages of real-time detection coupled with high spatial resolution as they rely only on low power optical transmission signals and thus have the potential for safe use *in-vivo*. In addition, the input radiation dose is proportional to the observed output fluorescence.

Fiber x-ray sensors can be classified as organic scintillator and inorganic scintillator based sensors according to the different scintillation materials used in their fabrication.[5–7] Organic scintillator materials have recently attracted much attention primarily due to their water equivalence. However, many of the organic scintillator materials are based purely on plastics, have a relatively low conversion efficiency (compared to inorganic materials) and hence often require the use of an additional fiber measurement channel to remove the influence of Cherenkov radiation.[8,9]

The fiber x-ray sensor comprising inorganic scintillators

*Project supported by the Natural Science Foundation of Heilongjiang Province, China (Grant No. ZD2019H003), the Joint Research Fund in Astronomy under Cooperative Agreement Between the National Natural Science Foundation of China and Chinese Academy of Sciences (Grant Nos. U1631239 and U1931206), the 111 Project, China (Grant No. B13015), and the Fundamental Research Funds for the Central Universities to the Harbin Engineering University, China.

†Corresponding author. E-mail: sunweimin@hrbeu.edu.cn

© 2021 Chinese Physical Society and IOP Publishing Ltd

generally has a better light output efficiency[10] than the corresponding organic version. The inorganic scintillator-based fiber x-ray sensor does not require additional fibers to remove the Cherenkov effect as it makes an insignificant contribution to the output light signal. Of many inorganic scintillators, the Gd_2O_2S:Tb is the material with the greatest potential to be used because of the combination of relatively high output intensity and extremely good linearity over the entire range of dose rate.[11] Therefore, the research of this paper is based on Gd_2O_2S:Tb fiber x-ray sensor. However, inorganic fiber x-ray sensor exhibits the over-response phenomenon, which means that the percentage dose depth (PDD) of the fiber x-ray sensor is larger than that of the gold standard IC detector at the deeper water depth in a water phantom.[3,5,12] However, the reason for the over-response phenomenon of the fiber x-ray sensor is still inconclusive. In addition, because of the over-response phenomenon, the application of fiber x-ray sensor is hindered. The research on over-response phenomenon has attracted the attention of many people.

Monte Carlo (MC) simulation is capable of providing detailed characteristics of incident photon beams for different field sizes and beam energy, and has already been applied to medical physics.[13,14] Martinez *et al.*[15] used the MC software PENELOPE and simplified the fiber probe into an 8-mm^3 cube, and considered that the over-response is due to the influence of the high effective atomic number, which increases the sensitivity of the detector to secondary radiation. Alharbi *et al.*[16] used the MC software EGSnrc to study the over-response phenomenon, but the simulation results were different from the experimental results, so they thought that the over-response is attributed to the influence of Cherenkov radiation. However, due to the limitations of the above-mentioned simulation software, they could not account for the light transport or, in some cases by using non-validated or not fully disclosed optical models.[17] Therefore, the above simulation tools cannot exactly match the experimental conditions.

In this article, the over-response phenomenon of the fiber x-ray sensor which makes uses of the inorganic scintillator Gd_2O_2S:Tb[18] is simulated by using the Monte Carlo (MC) based simulation software GEANT4.[19] Compared with previous MC simulation of fiber x-ray sensors, in this work the GEANT4 is used to simulate the fluorescence and Cerenkov radiation, and optical transmission inside the fiber, thus making the simulation conditions more realistic. This research will help us to understand the working mechanism of the fiber x-ray sensor through the study of the over-response phenomenon of the fiber x-ray detector, and has certain reference significance for future probe design and data acquisition.

2. Method

2.1. Experimental setup and results

A series of experiments was conducted at the clinic of the First Affiliated Hospital of Harbin Medical University. The medical accelerator used in the experiment was a Varian IX 3037. The inorganic scintillator material used in the fiber x-ray sensors was Gd_2O_2S:Tb, and the optical fiber was the SH2001-J (ESKA) PMMA plastic optical fiber. At the end of the PMMA fiber was drilled a hole with in diameter and 2 mm in depth. The Gd_2O_2S:Tb powder was filled into the hole. The fiber probe was placed in a water phantom, and the fluorescence was excited by irradiation from the x-rays of the medical accelerator. A Hamamatsu C11208-350 multi-pixel photon counting (MPPC) detector was used to monitor the intensity of fluorescence in real-time following transmission through a 25-m-long PMMA fiber. An IC (PTW30012) was used as a reference radiation dose measurement in the water phantom. The experimental setup is shown schematically in Fig. 1. The PDD curves of IC and the fiber x-ray sensor are shown in Fig. 2.

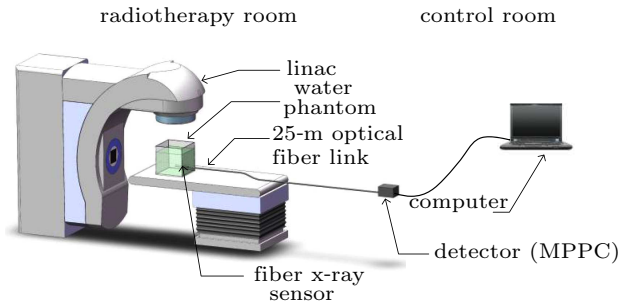


Fig. 1. Experimental setup.

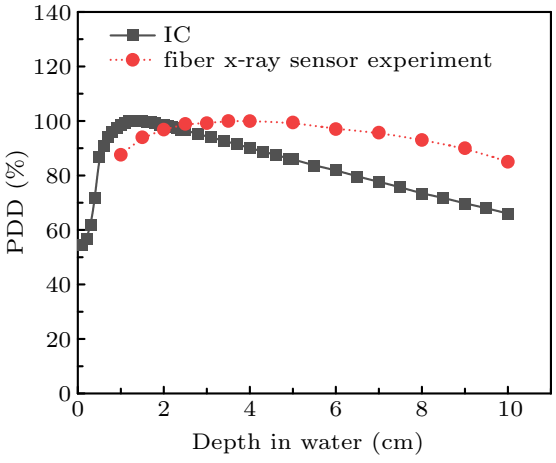


Fig. 2. Experimental result.

The PDD curve is an important characteristic of accelerator x-ray tissue penetration.[20] It can be seen from Fig. 2 that the measurement result of PDD of the fiber x-ray sensor is larger than that of the IC in the deeper water depth (4 cm–10 cm). Therefore, this article uses the Monte Carlo simulation software GEANT4 to conduct Monte Carlo simulation

research on fiber x-ray sensor to explore the causes of over-response phenomenon and the working mechanism of fiber x-ray sensor.

2.2. Monte Carlo simulation

The Monte Carlo simulations are based on the GEANT4 (GEometry ANd Tracking) simulation toolkit. The GEANT4 can trace most physical particles, and has therefore been widely used as a valuable tool in radiotherapy.[21]

The IAEA phase-space (phsp) format has been designed and agreed by an international expert committee for its medical applications.[22] Such a format has been implemented in recently released general-purpose MC code including EGSnrc and PENELOPE.[23] The GEANT4 is widely recognized as a state-of-the-art simulation toolkit for the coupled electron-photon transport in medical applications. And GEANT4 also contains a comprehensive range of physics models for electromagnetic, hadronic and optical interactions of a large set of particles over a wide energy range.[24]

Therefore, in this paper, the phsp file provided by the IAEA is used as a ray source model. The phsp model is based on a Varian IX source (VarianClinaciX_6MV_10x10_w1), delivering a ray energy of 6 MV, with a irradiation field dimension of 10 cm×10 cm.[25,26]

In the simulation, the water phantom was represented by a 30 cm×30 cm×30 cm cube as shown in Fig. 3(a), which is filled with G4_WATER. The fiber x-ray sensor probe was divided into two parts: the optical fiber itself and the scintillator, Gd_2O_2S:Tb.

(i) The PMMA fiber comprises a jacket, a cladding, and a core. The jacket is a 1-mm-diameter cylinder, and its material is polyethylene, and the length used is 13 cm. The core diameter is 485 μm, and the core material is PMMA, whose refractive index is 1.49. The cladding is an annular layer surrounding the core with 500 μm in diameter, and its material is fluorinated polymer, and its refractive index is 1.40.

(ii) The scintillator Gd_2O_2S:Tb fills an inner cylinder of 400 μm in diameter within the core of 2 mm in length as shown in Fig. 3(b).

At the other end of the PMMA fiber, a cylinder as shown in Fig. 3(c) was set up in the simulation in order to receive and count the number of photons generated by fluorescence and Cherenkov radiation.

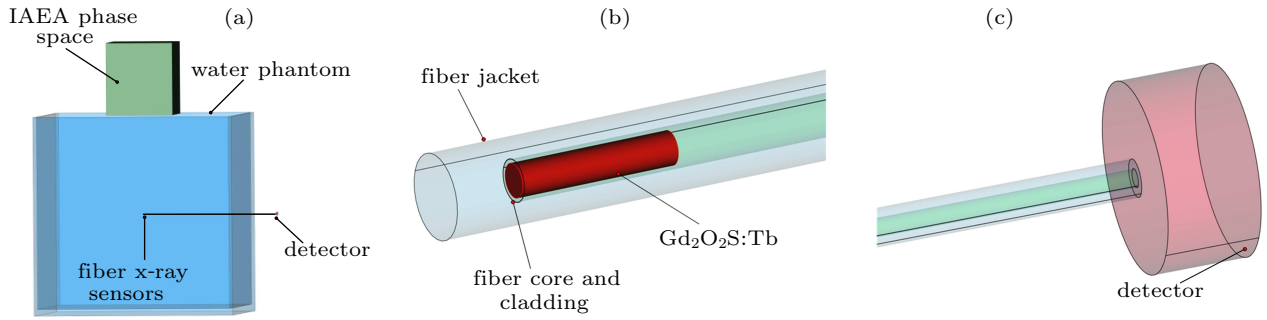


Fig. 3. (a) Simulation model setup consisting of four parts: phsp source, water phantom, fiber x-ray sensors, and detector; (b) fiber x-ray sensor structure; (c) detector for counting the number of photons transmitted through optical fiber.

2.3. Simulation parameters and data processing

In the case of GEANT4, the fluorescent properties of a scintillator comprise a light yield, a fluorescence wavelength, an absorption length, and decay time. In this simulation, two optical processes were considered, *i.e.*, Cherenkov radiation process and scintillation process. The basic physical process used in this simulation is G4EmStandardPhysics_option4, and the optical physics process (G4OpticalPhysics) is also investigated.

Previously reported research[16] indicated that the over response phenomenon is caused by Cherenkov radiation. Due to the existence of the optically opaque fiber jacket, the contribution of Cerenkov radiation generated from the water in the phantom can be ignored and the only contribution arising from Cerenkov radiation is that generated internally within the fiber. Therefore, when using GEANT4 to add the attributes to the fiber core and cladding material, the Cherenkov process is also considered naturally.

The contribution from the inorganic scintillation material, Gd_2O_2S:Tb is significant, and hence the inorganic scintillator is at the core for both the experiment and simulation. A series of parameters of the scintillator derived from the existing literature is set in the simulation, including the light yield (70000 MeV), the density (7.3 g/cm^3), the fluorescence wavelength (545 nm), and the decay time (1×10^6 ns).[27,28]

The CPU used for the simulation is an AMD Ryzen 2700, and the version of GEANT4 used is version 10.06 p01. The number of events is 6×10^7.

3. Simulation and analysis

3.1. PDD curves

By sequentially moving the fiber x-ray sensors on the central axis of the phantom, the number of fluorescent photons and Cherenkov photons generated by the fiber x-ray sensors

at different depths are extracted. The simulation and experimental results of the fiber x-ray sensor are shown together in Fig. 4.

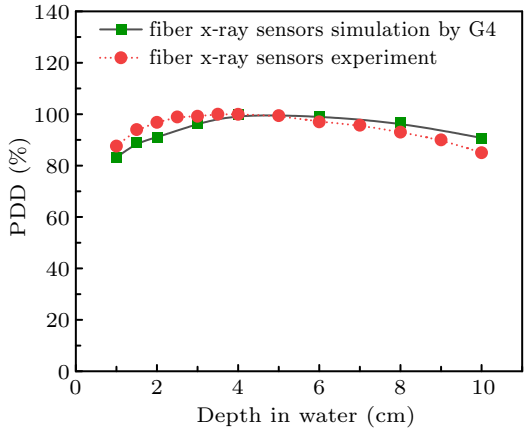


Fig. 4. Simulated and experimental PDD curves.

The experimentally obtained PDD from the fiber x-ray sensors shows that the maximum dose of the PDD curve occurs at around 4 cm. The MC simulation results obtained by using GEANT4 are close to the experimental results, in which the maximum dose depth is at around 4 cm–5 cm.

The over-response phenomenon of fiber x-ray sensors using inorganic scintillator materials has been widely investigated in previous literature. In some reports it was considered that the primary reason for its existence is that the inorganic materials have a larger number of atoms,[15] while in other reports it was considered that it was due to Cherenkov radiation,[16,29] and in some other reports it was proposed that it be due to the sensor material's response to different particle's energy.[12] Martínez *et al.*[15] used PENELOPE to simulate the fiber x-ray sensors based on filling the sensor with a YVO_4:Eu^{3+} crystal, and simplified the scintillator geometry into a 8-mm^3 cube. The simulation results of Martinez *et al.* showed that the over-response phenomenon appears to be the same as the experimental results of the fiber x-ray sensors. Martínez *et al.* attributed the over-response to the high Z_{eff} of the YVO_4:Eu^{3+}, which increases the sensitivity to secondary radiation. Alharbi *et al.*[16] also used Gd_2O_2S:Tb as an inorganic scintillator and carried out MC simulation experiments by using EGSnrc. The scintillator geometry was simplified into a 1-mm^3 cube. The results showed that when the field size was 10 cm×10 cm and the irradiation energy was 6 MV, the simulation results were similar to the IC data, and there appeared to be no over-response. Therefore, Alharbi *et al.* proposed that Cherenkov radiation have an effect on the over-response phenomenon. In their latest research, they modified the volume of the scintillator from 1 mm×1 mm×1 mm to 1 mm×1 mm×7 mm, under the same conditions, and the simulation results showed a slight over-response phenomenon.[29]

By comparing with the previous fiber x-ray sensor using Gd_2O_2S:Tb through Monte Carlo simulation,[16] where the deposition dose is represented by the extracted data, it can be seen that the deposition energy of the fiber x-ray sensor is not linearly related to its emitting fluorescence, which, therefore, is believed to be one of the reasons for the over-response phenomenon of the fiber x-ray sensor using Gd_2O_2S:Tb.

In the investigation of this article, the PDD simulation result shows an over-response phenomenon which is closely consistent with the experimental result. However, it does not fully comply with the experimental results, especially at the extreme depth: very shallow or very deep. The difference between simulation and experiment mainly comes from the modeling of the Linac source, that is, the phase space file in this article. Due to the possible deviation in the accelerator manufacturing process and the influence of the use environment, although its QA conforms to the standard, the fiber x-ray sensor is more sensitive to the particle energy, which leads to the difference between simulation and experiment.

The influence of Cherenkov radiation on the over-response phenomenon will be discussed in Subsection 3.2. In addition, another contribution to the over-response of the fiber x-ray sensor will be explained in Subsection 3.3.

3.2. Effect of Cherenkov radiation

In the process of modeling the fiber x-ray sensors in this investigation, the Cherenkov process is added. Therefore, in the simulated fiber x-ray sensors, the Cherenkov photons generated in the fiber at different water depths can be separately assessed, and the result is shown in Fig. 5.

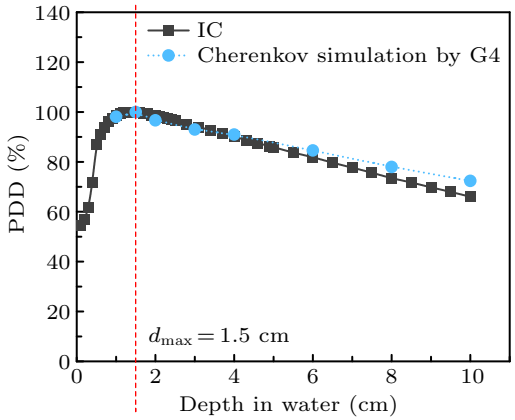


Fig. 5. Simulation results of Cherenkov radiation at different water depths compared with experimentally captured IC data.

The result of Fig. 5 shows that the PDD of the simulated Cherenkov radiation is similar to that obtained experimentally by using the IC. That is to say, Cherenkov radiation does not significantly contribute to the over-response phenomenon of fiber x-ray sensors when using inorganic scintillators. The maximum difference is 10% at 10 cm in depth which differs slightly from the previous MC simulation result of Cherenkov

radiation using "plain fiber".[30] The main reason for the difference is that the fiber length used in the previous article is shorter (5 cm) than the fiber used in this simulation (13 cm). In addition, Jang *et al.*[30] did not involve any influence of the fiber geometry.

When the number of simulated events is 6×10^7, the number of fluorescence photons and Cherenkov radiation photons received by the detector after transmission through the optical fiber are counted and shown in Table 1, and the ratio of the scintillation fluorescence of the inorganic scintillator received by the detector to the Cherenkov radiation is also calculated. The results show that the scintillation fluorescence is more than 900 times of Cerenkov radiation, and it also means that the Cherenkov inside the fiber contributes little to the over-response of the fiber x-ray sensors. Previous literature has shown that the signal measured by the fiber x-ray sensors is 735 times greater in magnitude than the Cerenkov signal at a depth of 2 cm[31] in water. The reason for the slight difference between the simulation result and the experimental result could be attributed to the fluorescent yield of the scintillator set during simulation being slightly different from the real value of the experimental situation, and a small difference in the length of the fiber. Therefore, based on the MC simulation of this investigation and previous literature, the contribution from the Cherenkov radiation from the inside of the fiber x-ray sensor using inorganic scintillators can be ignored.

Table 1. GEANT4-simulation-obtained number of fluorescence photons and Cerenkov radiation photons recorded by detector after transmission through optical fiber, and ratio of scintillation fluorescence (Fluo) to Cherenkov (Chko) in a depth range from 1 cm to 10 cm in water phantom.

Depth (cm)	1	1.5	2	3	4	6	8	10
Fluo (10^7)	2.033	2.175	2.224	2.357	2.446	2.427	2.366	2.220
Chko (10^4)	2.109	2.150	2.078	1.999	1.955	1.819	1.676	1.556
Fluo/Chko	964	1012	1070	1179	1251	1334	1411	1427

3.3. Interesting region

Fluorescence occurs due to energy deposition, while energy is deposited in the crystal by ionizing the charged particles or by converting the photons into electrons or positrons. The energy deposition of charged particles traversing scintillating materials causes the electrons to excite to higher energy states. In the course of the de-excitation, this energy is emitted in the form of visible photons and thus transferring into detectable light.[32] The objective of using the fiber x-ray sensors is to measure the real-time change of dose, the dose being derived from the deposition of charged particles, as the main working material of the fiber x-ray sensor of this investigation is inorganic scintillator (Gd_2O_2S:Tb) of effective atomic number $Z_{\rm eff} = 59.5$.[33] This material can respond to both x-rays and electrons. Ideally, the fiber x-ray sensor should be "transparent", however, in the mixed (including x-rays and secondary generated electrons) environment of the water phantom, x-rays become an external excitation source.

Due to the penetration depth of x-rays, not all x-ray photons in the water phantom will affect the fiber x-ray sensor. In this study, a region of interest is established to analyze the x-ray energy spectrum distribution, which helps to explain the reason for the existence of the over-response phenomenon of fiber x-ray sensors.

In order to describe the area of interest, using the concept of linear attenuation coefficient, the following formula is adopted:[34]

$$I = I_0\,\mathrm{e}^{-\mu x}, \tag{1}$$

where I is the intensity of photons transmitted at some distance x in the material, and I_0 is the initial light intensity, and μ is the linear attenuation coefficient. To simplify the model, a region of interest is defined as a sphere with a radius R. When the photon energy decays to half of it, $I = I_0/2$, the half-value layer (HVL); the thickness t can be calculated from

$$\frac{1}{2}I_0 = I_0\,\mathrm{e}^{-\mu x}, \tag{2}$$

$$x = \frac{\ln 2}{\mu} = \frac{0.693}{\mu}. \tag{3}$$

The mass thickness x is defined as the mass per unit area, and is obtained by multiplying the thickness t by the density ρ, so the HVL is $t = x/\rho$. The radius (R) of the sphere which represents the area of interest is equal to t. The sphere is shown schematically in Fig. 6.

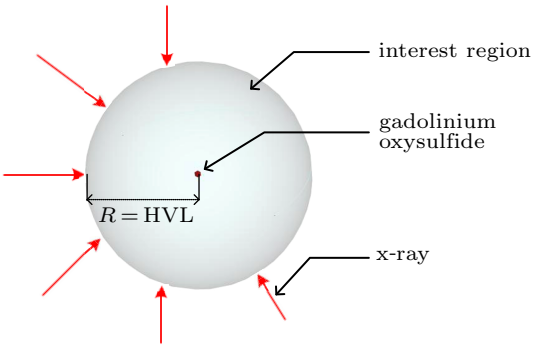


Fig. 6. Schematic representation of area of interest used in simulation of fluorescence from scintillation material.

The Gd_2O_2S:Tb used in the fiber x-ray sensor has previously been simplified into a 1-mm^3 cube.[16] If the energy of x-rays is high, the HVL of the "cube" will be larger than 1 mm, the x-rays will pass through the "cube" without losing much energy. From the formulae (1)–(3), it is possible to obtain a value $\mu/\rho = 0.94$ (cm^2/g). According to the NIST

website data,[34] the corresponding energy is about 150 keV. That means that the intensity of the x-ray is attenuated to half of it after penetrating a 1-mm-thick layer of Gd_2O_2S:Tb, if its energy is 150 keV. When the x-ray energy is greater than 150 keV, there is a certain probability with which the x-ray completely penetrates fiber x-ray sensor. Since in the PDD experiment the Gd_2O_2S:Tb is surrounded by water, and in order to reduce the radius of the region of interest as much as possible, the HVL of x-ray energy equal to 150 keV in water is also used as the radius of the region of interest. Using formula (3) and website data, in the water the ratio $\mu/\rho = 0.15$ $(\mathrm{cm}^2/\mathrm{g})$ is obtained and the radius (R) of the region of interest is calculated to be 4.6 cm. The GEANT4 counts the number of particles of various energy values in the region of interest to form an x-ray energy spectrum, which is shown in Fig. 7.

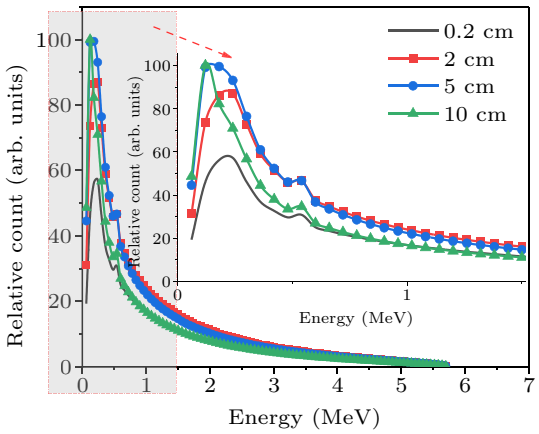


Fig. 7. The x-ray spectral distribution in region of interest at different water depths.

The results show that the x-ray energy spectrum in the region of interest gradually approaches to the lower energy region when the position of fiber x-ray sensor is deeper in the water phantom. This is mainly because the x-ray collides with the matter and the energy is reduced.

The central position of the interesting region, where the fiber x-ray sensor is located, is set separately at a depth of 0.2 cm, 2 cm, 5 cm, and 10 cm. The results show that if the position of the fiber x-ray sensor is deeper, the number of x-rays in the region of interest increases. When the central point of the region of interest ranges from 0.2 cm to 5 cm, the overall number of x-rays will increase, so the number of x-rays that generate the additional response to the fiber x-ray sensor increases. Therefore, theoretically, the measurement result of the fiber x-ray sensor should gradually increase in a range from 0.2 cm to 5 cm. This inference is very close to our simulation and experimental results. The maximum of PDD of our simulation is at the depth of 5 cm, and the maximum measured experimentally is also at 3 cm–4 cm. Before reaching the maximum dose point, the measured value gradually increases.

The x-ray beam from the Linac head has relatively high energy and can directly pass through the area of interest at the shallower depths (such as 0.2 cm), therefore, no counting occurs at these depths. When the fiber x-ray sensor position becomes deeper (say, in a range from 0.2 cm to 5 cm), the x-rays undergo various collisions in the water phantom, and the energy of the x-ray becomes smaller, and hence more x-rays are counted in the region of interest. Compared with the number of counts detected at a depth of 5 cm, the one at a depth of 10 cm is low. This is because the x-ray energy fluence continuously decreases with depth increasing, but when the maximum response depth value is exceeded, the response decreases as the water depth increases.

In addition, as shown in Fig. 7, the energy spectrum change is mainly concentrated in an area corresponding to the energy range from 0.1 MeV to 1.5 MeV. The inorganic scintillator Gd_2O_2S:Tb used in the fiber x-ray sensor of this investigation has a relatively large effective atomic number $Z_{\mathrm{eff}} = 59.5$. The photoelectric cross section is approximately proportional to $Z^{3.5}/E^3$, where E is the energy of the photon beam, and Z is the effective atomic number.[35] Therefore, the inorganic scintillator in the optical fiber x-ray sensor is more sensitive to low-energy x-ray particles.

In summary, it is proposed that the over-response of fiber x-ray sensors in this paper be mainly caused by the two effects as follows.

(i) The inorganic scintillator can respond to both x-rays and electrons. In the water phantom, there are some x-rays colliding with the inorganic scintillator part of the fiber x-ray sensor, which makes a certain contribution to the over-response phenomenon of fiber x-ray sensor.

(ii) Comparing with previous Monte Carlo simulation results, inorganic scintillator has a nonlinear relationship with the deposited energy, and fiber x-ray sensor may have a high response to photons in the low energy region.

Simulation results (Subsection 3.2) show that the contribution of the internally generated Cherenkov radiation (inside the optical fiber) to the over-response of fiber x-ray sensors can be ignored.

4. Conclusions

In this paper, the Monte Carlo simulation software GEANT4 is utilized to study the optical fiber sensor using an inorganic scintillator Gd_2O_2S:Tb. The over-response phenomenon of fiber x-ray sensor is simulated by GEANT4, and the simulation result is close to the experimental measurement. Through the extraction of Cherenkov radiation of fiber and the fluorescence optical data of the scintillator, it is found that the Cherenkov radiation does not make a significant contribution to the fiber x-ray sensor using inorganic scintillators. Finally, a model is established for the region of interest, which helps to explain the possible causes of the over-response by examining

the x-ray energy spectrum distribution in this region. However, this model is limited by the difference between the accelerator phsp file and the beam characteristics of the real Linac. In the follow-up work to be reported later, the calibration of the accelerator model and the study of the characteristics of the scintillator will be carried out.

References

[1] Nutting C, Dearnaley D P and Webb S 2000 *The British Journal of Radiology* **73** 459

[2] Wuerfel J U 2013 *Medical Physics International* **1** 81

[3] O'Keeffe S, Zhao W, Sun W, Zhang D, Qin Z, Chen Z, Ma Y and Lewis E 2016 *IEEE J. Select. Top. Quantum Electron.* **22** 35

[4] Sun W, Qin Z, Ma Y, Zhao W, Hu Y, Zhang D, Chen Z and Lewis E 2016 *Optical Sensing and Detection IV* (Brussels: Belgium), 98991D

[5] Qin Z, Hu Y, Ma Y, Lin W, Luo X, Zhao W, Sun W, Zhang D, Chen Z, Wang B and Lewis E 2016 *Biomed. Opt. Express* **7** 4919

[6] Beddar A S, Mackie T R and Attix F H 1992 *Phys. Med. Biology* **37** 1883

[7] Beddar A S, Mackie T R and Attix F H 1992 *Phys. Med. Biology* **37** 1901

[8] Guillot M, Beaulieu L, Archambault L, Beddar S and Gingras L 2011 *Med. Phys.* **38** 6763

[9] Archambault L, Beddar A S, Gingras L, Roy R and Beaulieu L 2005 *Med. Phys.* **33** 128

[10] Nicholas T and Landsberger 2015 *Measurement and Detection of Radiation* (CRC Press)

[11] Hu Y, Qin Z, Ma Y, Zhao W, Sun W, Zhang D, Chen Z, Wang B, Tian H and Lewis E 2018 *Sensors and Actuators A: Physical* **269** 188

[12] Qin Z, Xie T, Dai X, Zhang B, Ma Y, Khan I U, Zhang X, Li H, Yan Y, Zhao W, Li S, Chen Z, Zhang D, Xu J, Hu X, Xing L, Feng K, Lewis E and Sun W 2019 *Opt. Express* **27** 23693

[13] Ding G X 2002 *Phys. Med. Biology* **47** 1025

[14] Andreo P 1991 *Phys. Med. Biology* **36** 861

[15] Martínez N, Rucci A, Marcazzó J, Molina P, Santiago M and Cravero W 2017 *Radiation Measurements* **106** 650

[16] Alharbi M, Martyn M, Chen L, Gillespie S, Woulfe P, O'Keeffe S and Foley M 2018 *Optical Sensing and Detection V*, Strasbourg, France, 106800Z

[17] Roncali E, Mosleh-Shirazi M A and Badano A 2017 *Phys. Med. Biol.* **62** R207

[18] Gorokhova E I, Demidenko V A, Mikhrin S B, Rodnyi P A and van Eijk C W E 2005 *IEEE Trans. Nucl. Sci.* **52** 3129

[19] Allison J, Amako K, Apostolakis J, *et al.* 2006 *IEEE Trans. Nucl. Sci.* **53** 270

[20] Ahnesjo A and Aspradakis M M 1999 *Phys. Med. Biology* **44** R99

[21] Archambault L, Polf J C, Beaulieu L and Beddar S 2008 *Phys. Med. Biology* **53** 1865

[22] Cortés-Giraldo M A, Quesada J M, Gallardo M I and Capote R 2012 *International Journal of Radiation Biology* **88** 200

[23] Rucci A, Carletti C, Cravero W and Strbac B 2014 *Physica Medica* **30** 242

[24] Maigne L, Perrot Y, Schaart D R, Donnarieix D and Breton V 2011 *Phys. Med. Biology* **56** 811

[25] Cortes-Giraldo M A, Quesada J M, Gallardo M I and Capote R *Geant interface to work with IAEA phase-space files*

[26] Rodrigues A, Sawkey D, Yin F F and Wu Q 2015 *Med. Phys.* **42** 2389

[27] Weber M J 2002 *J. Luminescence* **100** 35

[28] Carel W E van Eijk 2002 *Phys. Med. Biol.* **47** R85

[29] Alharbi M, Martyn M, O'Keeffe S, Therriault-Proulx F, Beaulieu L and Foley M 2019 *Phys. Med.* **68** 124

[30] Jang K W, Yagi T, Pyeon C H, Yoo W J, Shin S H, Jeong C, Min B J, Shin D, Misawa T and Lee B 2013 *J. Biomed. Opt.* **18** 27001

[31] Zhuang Q, Yaosheng H, Yu M, Wenhui Z, Weimin S, Daxin Z, Ziyin C and Elfed L 2016 *Opt. Express* **24** 5172

[32] Dietz-Laursonn E 2016 *Detailed Studies of Light Transport in Optical Components of Particle Detectors*, Ph. D. Dissertation (Aachen, Tech. Hochsch)

[33] Stock S R 2008 *MicroComputed Tomography: Methodology and Applications*

[34] Hubbell J H and Seltzer S M 2004 *Tables of X-Ray Mass Attenuation Coefficients and Mass Energy-Absorption Coefficients* (version 1.4)

[35] Agyingi E O, Mobit P N and Sandison G A 2006 *Radiation Protection Dosimetry* **118** 28